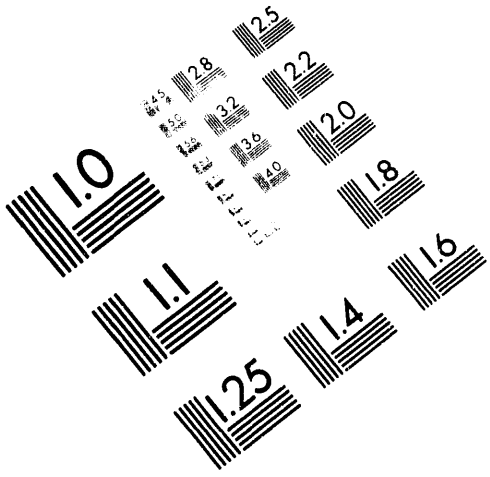

Association for Information and Image Management
1100 Wayne Avenue, Suite 1100
Silver Spring, Maryland 20910
301/587-8202

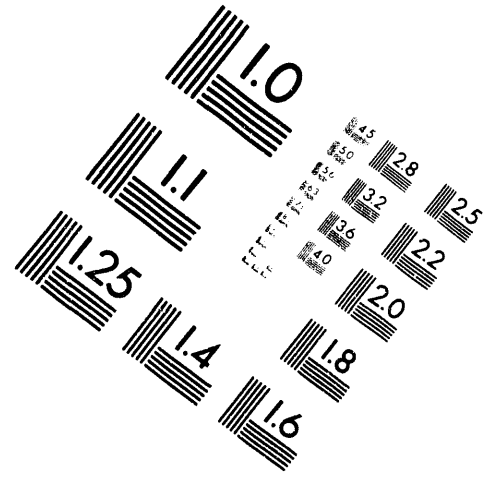

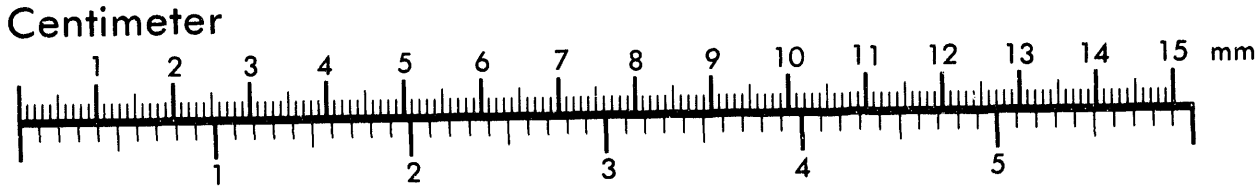

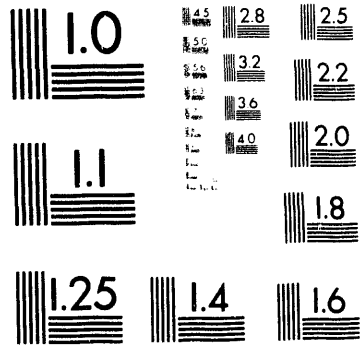

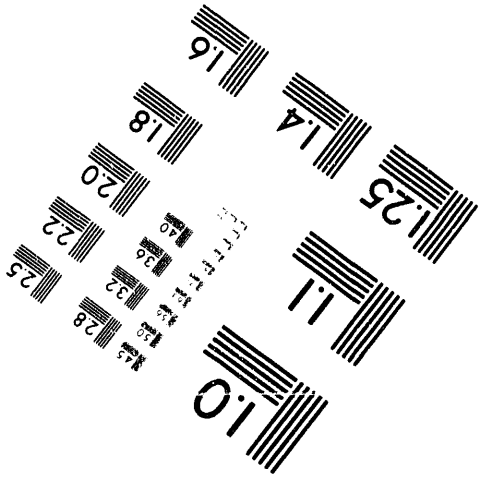

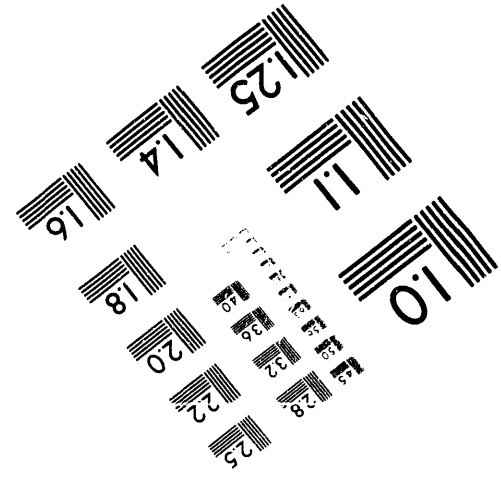

MANUFACTURED TO AIIM STANDARDS
BY APPLIED IMAGE, INC.

1 of 1

An Experimental and Theoretical Study to Relate Uncommon Rock/Fluid Properties to Oil Recovery

QUARTERLY REPORT FOR THE PERIOD

October 1, 1992 Through December 31, 1992

Prepared by
Robert W. Watson, Turgay Ertekin and Olubunmi O. Owolabi

The Pennsylvania State University
College of Earth & Mineral Sciences
Mineral Engineering Department
Petroleum & Natural Gas Engineering Section
102 Mineral Sciences Building
University Park, PA 16802

Prepared for

U.S. Department of Energy
Bartlesville Project Office
Under Contract No. DE-AC22-89BC14477

DOE Project Manager
Gene Pauling

US/DOE patent clearance is not required prior to the publication of this document.

TABLE OF CONTENTS

RESEARCH SUMMARY

TITLE:	An Experimental and Theoretical Study to Relate Uncommon Rock/Fluid Properties to Oil Recovery
CONTRACT:	DE-AC22-89BC14477
CONTRACTOR:	The Pennsylvania State University Vice President for Research 114 Kern Building University Park, PA 16802 Administrative Officer: David A. Shirley
PRINCIPAL INVESTIGATOR:	Robert W. Watson Assistant Professor Petroleum and Natural Gas Engineering 102 Mineral Sciences Building University Park, PA 16802
REPORTING PERIOD:	October 1, 1992-December 31, 1992

MAJOR ACHIEVEMENTS

The major objectives of the current quarter are to complete the porosimetry experiments and to analyze the experimental data on 512 plugs that were extracted from 16 waterflooded Indiana limestone linear-cores. The plugs were previously tested for their

References and Illustrations at end of paper.

wettability indices and then cleaned in readiness for the mercury porosimetry tests.

OVERALL PROJECT OBJECTIVES

The overall objectives of the project are:

- To develop a better understanding of some important but not really well investigated rock/pore properties such as: tortuosity, pore-size distribution, surface area, and wettability, and a better insight on capillary pressure variation with respect to wettability and pore geometry of sandstone and limestone.
- To improve the understanding of fluid flow in porous media under conditions of secondary and tertiary recovery, through the laboratory study of the performance of enhanced recovery methods such as waterflooding.
- To develop empirical relationships between residual oil saturation and oil recovery at breakthrough and the uncommon rock/pore properties. Develop relationships between residual oil saturation and ultimate oil recovery at floodout and the uncommon rock/pore properties for the different porous media. Furthermore, variations of irreducible water saturation, porosity and absolute permeability with respect to the uncommon rock/pore properties, residual oil saturation and oil recovery will be investigated.

ACTUAL WORK-PREVIOUS QUARTER

During the previous quarter, waterflooding experiments and wettability experiments were completed on 16 Indiana limestone linear cores and 512 core plugs. The influence of microscopic rock-pore characteristics such as tortuosity, wettability, and irreducible water saturation on residual oil saturation and ultimate oil recovery was thoroughly investigated.

The properties were analyzed at both the breakthrough and floodout periods.

WORK PLANNED-CURRENT QUARTER

Plans for the current quarter consist of the following:

- Complete the mercury porosimetry experimental studies on the Indiana limestone linear cores and analyze the results.
- Relate mercury recovery efficiency, mercury residual saturation, porosity, total intrusion volume, pore surface area, pore diameter, skeletal density and the other mercury porosimetry properties to each other.
- The trends exhibited by the properties investigated are to be compared with the previously analyzed waterflooding and wettability experimental results.
- Study the statistical distribution of the mercury porosimetry properties in Indiana limestone co .s.
- Experimentally and statistically describe the above mentioned variables, with the aim of developing empirical models to improve the prediction of oil recovery resulting from waterflooding for limestone reservoirs.

ACTUAL WORK-CURRENT QUARTER

During the current quarter, the mercury porosimetry experiments on limestone core-plug samples were completed. The experimental data were also fully analyzed.

INTRODUCTION

One of the most important component of reservoir characterization is the description of the pore systems, which is one of the factors that control the production potential of the reservoir. Pore systems are studied by a family of methods called petrophysical analysis; one of these methods is mercury porosimetry (Kopaska-Merkel and Friedman, 1989). In this method, mercury is injected into the pore system of a sample under controlled conditions, to produce capillary pressure curves.

Mercury porosimetry analysis for the identification of petrophysical properties is a relatively rapid procedure (Ghosh and Friedman, 1989). Capillary pressure data from mercury porosimetry are used to determine petrophysical characteristics such as total intrusion volume, pore surface area, median and average pore diameter, porosity, residual mercury saturation and mercury recovery efficiency. Such petrophysical information is critical to all phases of reservoir exploitation, but especially enhanced recovery, which depends on accurate predictions of the behavior of fluids in rock Kopaska-Merkel and Amthor, 1988).

Lowell and Shields (1981) noted that the experimental method of mercury porosimetry for the determination of porous properties of solids is dependent on several variables such as wetting or contact angle between mercury and the surface of the solid.

EXPERIMENTAL PROCEDURE

Samples Cleaning

Prior to testing, all the 512 limestone core-plugs that were previously tested for wettability, were cleaned by soaking for 48 hours in solution containing 50% by volume acetone and 50% by volume isopropyl alcohol (IPA). This was followed by an additional

soaking for 24 hours in acetone solution only. Finally, the core plugs were dried in a vacuum oven for 24 hours at a temperature of 60°C.

Mercury Porosimetry Experiments

The experiments were carried out on a Micromeritics mercury porosimeter (Pore Sizer Model 9220). The samples were weighed and each installed in penetrometers. Four samples in penetrometers were installed in the low-pressure ports at a time and evacuated simultaneously in low pressure ports until a stabilized pressure of about 50 μm was obtained. Mercury was then allowed to fill the penetrometers and low-pressure tests were performed by permitting dry air to be admitted in discrete increments from 1.5 psia to 14 psia (about atmospheric pressure).

At the conclusion of the low pressure runs, the penetrometers containing mercury and samples were weighed and two of them were installed in the high-pressure chambers at a time. The high-pressure runs could be performed at specific values from 14 to 60,000 psia (air-mercury) by raising the pressure incrementally and allowing equilibration at each increment. With each increment of pressure, smaller pore throats were invaded by mercury. For this present study, the maximum pressure was limited to 11,000 psia, because the amount of mercury intrusion above this pressure is negligible for the types of samples being investigated. Kopaska-Merkel and Amthor (1988) pointed out that any capillary-pressure study done to evaluate reservoir rock should cover the pressure range corresponding to pressures which might be encountered in the subsurface (probably at least 10,000 psia) or one runs the risk of under-estimating available porosity by up to 30% or more.

Pore size information are obtained from mercury intrusion (drainage) curves based on the assumption of a cylindrical pore configuration. It is assumed that mercury is the non-wetting phase which displaces completely the wetting phase (mercury vapor or air) in the

rock samples. The extrusion (imbibition) curves are obtained by releasing pressure and recording equilibrated values and taking readings at successively lower pressures.

RESULTS AND DISCUSSIONS

Mercury Porosimetry Results

A total of 512 core plugs were extracted from along the flow path of the 16 waterflooded Indiana limestone linear-cores. These extracted plugs are the same that were previously tested for wettability and later cleaned in readiness for the mercury porosimetry tests. After the completion of low-pressure and high-pressure runs, the plugs were discarded because of being contaminated with mercury.

Similar to the analysis on the wettability data, average values of mercury porosimetry properties were obtained for each of the core samples from the core plugs and these values are presented in Table 1 for the types of mode, pore intrusion volumes, pore surface areas, pore specific surface areas, average pore diameters, apparent densities, mercury porosities, residual mercury saturations and mercury recovery efficiencies.

Table 2 shows the statistical description of the mercury porosimetry experimental data obtained. For all the core samples combined, intrusion volumes varied from 0.06 to 0.08 ml/g, with an average of 0.07 ml/g; the surface areas varied from 0.83 to 1.06 m^2/g, with an average of 0.93 m^2/g; the specific surface area varied from $12.48*10^4$ to $16.45*10^4$ cm^2/cm^3, with an average of $13.94*10^4$ cm^2/cm^3; the average pore diameters varied from 0.26 to 0.35 μm, with an average of 0.30 μm; the apparent (skeletal) densities varied from 2.55 to 2.65 g/ml, with an average of 2.60 g/ml; the porosities varied from 13.8 to 16.2%, with an average of 14.6%; the residual mercury saturations varied from 55.9 to 66.1%, with an average of 61.3%; and the mercury recovery efficiencies varied from 33.9 to 44.1%, with an average value of 38.8%.

The limestone rocks investigated are considered to be very good reservoir rocks because they have both high mercury recovery efficiency and porosity values. According to Kopaska-Merkel and Friedman (1989), mercury recovery efficiency in mercury porosimetry is analogous to primary recovery of petroleum from natural reservoirs because both processes involve only simple pressure reduction. Hence, this type of rock with more than 25% mercury recovery efficiencies and fairly good porosities, would perform well during primary oil recovery period.

Figures 1 through 7 show the distributions of the various mercury porosimetry properties of the limestone core plug samples. The properties are total intrusion volume, surface area, specific surface area, average pore diameter, apparent (skeletal) density, mercury porosity, and mercury recovery efficiency, respectively. For the distributions and subsequent analyses, only 329 out of the original 512 limestone core plugs were utilized, because of the removal of all the bad mercury porosimetry experimentally measured data.

The plots of the plugs mercury porosities versus the normalized distances for each of the 16 cores are presented in Figs. 8 through 15. Similar to the case of the wettability indices the exhibited trends are generally not constant. The reason for this is not fully understood, but might be related to the amount of microporosity within the fossil and oolite grains, and/or to the presence of clay fines in the core samples (Churcher et al., 1991).

The correlation matrix shown in Table 3 confirms the trends of Figs. 16 through 18. Figure 16 shows a good relationship between total intrusion volume and mercury porosity, with a R^2 value of about 52% and high F-test statistic value of 15.31. The relationship is statistically significant at $\alpha = 0.005$ level. Figure 17 show that mercury recovery efficiency have inverse relationship with the average pore diameter. A probable explanation for this relationship is that capillary trapping of the mercury by snap-off during extrusion is likely to be minimized in pore systems of small pore-throat size contrast (Wardlaw and Cassan,

1979). The relationship is strong with a significant value of 0.001. This is in agreement with the findings of Amthor et al. (1988), that for intermediate pore throat sizes, the mercury recovery efficiency are moderate for gently sloping bimodal systems.

Figure 18 shows that apparent (skeletal) density is directly proportional to total intrusion volume. The relationship is statistically significant at $\alpha = 0.1$ level. the relationship between mercury recovery efficiency and porosity was found not to be statistically significant ($R = -0.29$), as shown in the correlation matrix of Table 3. Review of the literature also depict that apparently no one consistent set of relationships exists between mercury recovery efficiency and porosity for carbonate rocks. Inversely proportional relationship was found by Amthor et al. (1988) and Kopaska-Merkel and Friedman (1989). Contrary to these findings, Wardlaw (1976), Ghosh and Friedman (1989), and Al-Fossail et al. (1991), found a directly proportional relationship between mercury recovery efficiency and porosity of carbonate rock samples.

Relation Between Porosimetry and Petrophysical Properties

Correlation matrices for the full models at breakthrough and floodout for limestones were investigated and presented in Tables 4 and 5, respectively. The agreement between porosity values obtained using mercury porosimetry and those obtained from the corefloods were good as shown in Fig. 19. It was observed that if a 45° degree line is drawn on the plot, 11 of the data points lie above the line and the other five are close to the 45° line. This finding tells us is that the brine porosities were larger than the mercury porosities. This is in agreement with the what was observed for the case of sandstone core samples.

The relationship of brine permeability versus total intrusion volume is presented in Fig. 20. The relationship is directly proportional with a standard deviation of 2.9 md, F-test statistic of 5.94, and statistically significant at $\alpha = 0.05$ level. All the other relationships of petrophysical properties with total intrusion volume failed the significance tests, as shown in

the correlation matrices presented in Tables 4 and 5. These tables are further employed to analyze the relationships of mercury porosimetry properties with the other petrophysical properties. Except for the relationships of formation resistivity factor with specific surface area and average pore diameter, all the other petrophysical properties relationships with surface area, specific surface area, and average pore diameter, are not statistically significant. The specific surface area values of the limestone core samples investigated in this study, are considerably higher than those obtained for the sandstones ($12.48*10^4$ to $16.45*10^4$ versus $1.84*10^4$ to $8.58*10^4$ cm^2/cm^3). Permeability is directly proportional to apparent (skeletal) density and it has an inversely proportional relationship with mercury recovery efficiency. Tortuosity has an inversely proportional relationship with apparent (skeletal) density and directly proportional relationship with mercury recovery efficiency. The relationship of formation resistivity factor with specific surface area is directly proportional. Formation resistivity factor has inversely proportional relationships with average pore diameter and apparent (skeletal) density.

Relation Between Porosimetry and Waterflood Properties

The limestones mercury porosimetry properties were individually related to the residual oil saturation and oil recovery at breakthrough and at floodout, as presented in the correlation matrices of Tables 4 and 5, respectively. At breakthrough, unlike in the case of sandstones, all the relationships except those of surface area with residual oil saturation and oil recovery, were observed to be statistically significant at $\alpha = 0.1$ level. At floodout, apart from the relationships of total intrusion volume and mercury porosity with residual oil saturation and oil recovery, the others failed the significance tests.

At both the breakthrough and floodout, the relationships of total intrusion volume with residual oil saturation are inversely proportional and its relationships with oil recovery are directly proportional. Residual oil saturation at breakthrough is directly proportional to

specific surface area and mercury recovery efficiency, but inversely proportional to average pore diameter, apparent (skeletal) density, and mercury porosity. In the case of oil recovery at breakthrough, it is inversely proportional to specific surface area and mercury recovery efficiency, but directly proportional to average pore diameter, apparent (skeletal) density, and mercury porosity.

Relation Between Porosimetry and Wettability Properties

The relationships of average wettability index with the various mercury porosimetry properties were investigated, as shown in the correlation matrices of Tables 4 and 5. All of the mercury porosimetry properties show relationships that are not statistically significant with average wettability index.

Shape of the Capillary Pressure Curve

Capillary-pressure curves reflect the capillary forces which govern the distribution of fluids in the porous system and influence the flow of fluids. The shapes of the capillary-pressure curves do not appear to be a unique function of either sandstones or limestones, but mainly reflect the pore size distribution in the rock. Figure 21 presents the capillary-pressure versus cumulative mercury intrusion/extrusion curve for plug 28 of sample core 15B. Similar to most of the other Indiana limestone core plug samples investigated in this study, the mode type of the curve is bimodal with gently-sloping shape. This is further confirmed in Fig. 22, which is the plot of capillary-pressure versus incremental mercury intrusion/extrusion curve for the same plug.

The existence of multiple modes is significant because it affects the overall non-wetting-phase recovery efficiency. For the investigated limestone samples, the gently slopping bimodal curves correlate with high mercury recovery efficiency (mean = 39%), high porosity (mean = 15%), intermediate average pore diameter (mean = 0.30 μm), and

high entry pressures. The capillary-pressure versus cumulative pore area curve for the plug is presented in Fig. 5.23. Only the mercury intrusion data were used to plot Fig. 5.23.

Churcher et al. (1991) also observed bimodal capillary-pressure curve shapes in their previous studies using Indiana limestone core samples. They suggested that the bimodal pore throat size distributions in Indiana limestone samples may result from the distribution of the fine calcite crystals which line the pores and create microporosity. They were also of the opinion that it may also arise from the intra-particle porosity noted in some fragments and oolites.

In the report of their studies on the reservoir characterization of deeply-buried paleozoic carbonates from Oklahoma, Texas and New Mexico, Amthor et al. (1988) argued that the shapes of capillary-pressure curves are useful components of a formal classification of carbonate rocks. The simple empirical classification of capillary-pressure curves allows evaluation of potential of potential reservoir rocks at a glance in terms of their petrophysical properties. They further postulated that steep-convex capillary-pressure curves indicate reservoir rocks with high recovery efficiencies, but low porosities and small throats, so that the production is likely to be economical only under high pressures (or thick oil columns) or from very large hydrocarbon pools. Conversely, steep-concave curves indicate porous reservoir rocks with large throats but probably poor primary recovery efficiency. These reservoirs will be economical even at low pressures and with short oil columns and small total reserves, but will probably need enhanced recovery to produce a significant proportion of the reserves. They suggested that gently-sloping curves correspond to samples with moderate recovery efficiencies, intermediate median throat sizes, and variable porosities. Polymodal curves result from polymodal throat-size distribution, and exhibit variable recovery efficiencies and porosities.

PROBLEMS ENCOUNTERED

No technical problems were encountered.

WORK PLANNED-NEXT QUARTER

Plans for the next quarter consist of the following:

- Develop new correlations for estimating mercury recovery efficiency values for sandstones and limestones.
- Develop new correlations for estimating permeability values for sandstones and limestones using mercury porosimetry measured data.
- Experimentally and statistically describe all the independent variables from waterflood, wettability and mercury porosimetry experiments to residual oil saturation and oil recovery, for limestones.

CONCLUSIONS

The following conclusions are deduced from this study:

- Mercury recovery efficiency exhibited inverse relationship with the average pore diameters.
- The mercury porosities obtained by averaging the plug values over a given core sample, are in agreement with those obtained from the waterflooding experiments. The porosities also correlated pretty well with the total intrusion volumes.
- Tortuosity has an inverse relationship with apparent (skeletal) density and directly proportional relationship with mercury recovery efficiency.

- Permeability is directly proportional to apparent (skeletal) density and it has an inversely proportional relationship with mercury recovery efficiency.
- The relationship of formation resistivity factor with specific surface area is directly proportional. Formation resistivity factor has inversely proportional relationships with average pore diameter and apparent (skeletal) density.
- The limestone cores investigated were all found to exhibit gently-sloping bimodal capillary pressure curve shapes.

NOMENCLATURE

B.T.	=	breakthrough time
d	=	capillary tube or pore diameter (micrometer)
$\overline{D}$	=	average pore diameter (micrometer)
F.O.	=	floodout time
Max.	=	maximum value of a particular data
Min.	=	minimum value of a particular data
mode 1	=	unimodal capillary pressure shape
P	=	pressure (psia)
P_c	=	capillary pressure (psia)
Q_1	=	lower quartile or first quartile
Q_3	=	upper quartile or third quartile
RE	=	mercury recovery efficiency (fraction)
SA	=	total Pore Area (or surface area) (sq. m/g)

S_{Hg}	=	mercury saturation (fraction)
S_r	=	residual mercury saturation (fraction)
S_s	=	specific surface area (cm^2/cm^3)
St. Dev.	=	standard deviation
V_B	=	bulk volume of sample (ml/g)
$V_{int.}$	=	total intrusion volume (or pore volume) (ml/g)
V_S	=	grain volume (ml/g)
ΔS_{Hg}	=	incremental change in mercury saturation
ρ_B	=	bulk density (g/ml)
ρ_s	=	apparent (skeletal) density (g/ml)
ϕ	=	porosity (fraction)
ϕ_{Hg}	=	mercury porosimetry measured porosity (fraction)
σ	=	surface tension for liquid (dyn/cm)
θ	=	contact angle for liquid on solid (deg.)

ACKNOWLEDGEMENTS

The authors wish to acknowledge the financial support of the U.S. Department of Energy to the Pennsylvania State University through Contract No. DE-AC22-89BC14477.

REFERENCES

Al-Fossail, K.A., Saner, S., Asar, H.K., and Hossain, M.: "Factor Affecting Mercury Capillary Pressure Behavior of Saudi Arabian Carbonate Reservoir Rocks," paper No. SPE 21434 presented at the 1991 SPE Middle East Oil Show, Bahrain, Nov.

16-19, 815-820.

Amthor, J.E., Kopaska-Merkel, D.C., and Friedman, G.M.: "Reservoir Characterization, Porosity, and Recovery Efficiency of Deeply-Buried Paleozoic Carbonates: Examples from Oklahoma, Texas and New Mexico," *Carbonates and Evaporites*, (1988), **3**, No. 1, 33-52.

Churcher, P.L., French, P.R., Shaw, J.C., and Schramm, L.L.: "Rock Properties of Berea Sandstone, Baker Dolomite, and Indiana Limestone," paper No. SPE 21044 presented at the 1991 SPE International Symposium on Oilfield Chemistry, Anaheim, CA., Feb. 20-22.

Ghosh, S.K., and Friedman, G.M.: "Petrophysics of a Dolostone Reservoir: San Andres Formation (Permian), West Texas," *Carbonates and Evaporites*, (1989), **4**, No. 1, 45-117.

Kopaska-Merkel, D.C., and Amthor, J.E.: "Very High-Pressure Mercury Porosimetry as a Tool in Reservoir Characterization," *Carbonates and Evaporites*, (1988), **3**, No. 1, 53-63.

Kopaska-Merkel, D.C., Friedman, G.M.: "Petrofacies Analysis of Carbonate Rocks: Example From Lower Paleozoic Hunton Group of Oklahoma and Texas," *AAPG Bull.*, (Nov. 1989), **73**, No. 11, 1289-1306.

Lowell, S., and Shields, J.E.: Powder Surface Area and Porosity, Chapman and Hall, New York, NY., 1981.

Wardlaw, N.C.: "Pore Geometry of Carbonate Rocks as Revealed by Pore Casts and Capillary Pressure," *AAPG Bull.*, (1976), **60**, 245-257.

Wardlaw, N.C., and Cassan, J.P.: "Oil Recovery Efficiency and the Rock-Pore Properties of some Sandstone Reservoirs," *AAPG Bull.*, (June 1979), **27**, No. 2, 117-138.

SI METRIC CONVERSION FACTORS

°API 141.5/(131.5+°API)	=	g/cm^3
bbl x 1.589 873 E-01	=	m^3
cp x 1.0* E+00	=	mPa.s
ft x 3.048* E-01	=	m
ft^3 x 2.831 685 E-02	=	m^3

°F (°F-32)/1.8	=	°C
gal x 3.785 412 E-03	=	m^3
in x 2.54* E+00	=	cm
lbm x 4.535 924 E-01	=	kg
psi x 6.894 757 E-01	=	kPa

*Conversion factor is exact.

Table 1: Mercury Porosimetry Properties of the Indiana Limestone Cores

Core Sample No.	No. of Plugs	Type of Mode	$V_{Int.}$ (ml/g)	SA (m^2/g)	S_o (cm^2/cm^3) (E+04)	$\bar{D}$ (μm)	ρ_o (g/ml)	ϕ_{Hg} (%)	S_r (%)	RE (%)
9A	32	2	0.0688	0.987	14.346	0.279	2.625	15.27	61.20	38.80
9B	32	2	0.0738	1.030	13.957	0.309	2.649	16.24	62.53	37.47
10A	32	2	0.0644	0.830	12.888	0.313	2.622	14.40	66.12	33.88
10B	32	2	0.0673	0.936	13.908	0.291	2.606	14.44	62.54	37.46
11A	32	2	0.0678	0.853	12.581	0.335	2.603	14.96	61.36	38.64
11B	32	2	0.0635	0.892	14.047	0.273	2.588	14.07	57.67	42.33
12A	32	2	0.0693	0.865	12.482	0.299	2.551	13.76	62.14	37.86
12B	32	2	0.0668	0.860	12.874	0.312	2.619	14.88	64.75	35.25
13A	32	2	0.0766	0.970	12.663	0.350	2.616	15.47	66.13	33.87
13B	32	2	0.0691	0.958	13.864	0.289	2.622	14.48	61.33	38.67
14A	32	2	0.0645	1.061	16.450	0.260	2.587	14.30	57.64	42.36
14B	32	2	0.0635	0.935	14.724	0.273	2.589	14.10	58.28	41.72
15A	32	2	0.0633	0.914	14.439	0.279	2.571	13.96	61.79	38.21
15B	32	2	0.0660	0.834	12.636	0.317	2.604	14.65	64.29	35.71
16A	32	2	0.0614	0.953	15.521	0.299	2.589	14.36	56.34	43.66
16B	32	2	0.0674	1.056	15.668	0.263	2.593	14.93	55.92	44.08

Table 2: Statistical Description of the Mercury Porosimetry Experimental Variables for Indiana Limestone Cores

	V_{Hg} (ml/g)	SA (m^2/g)	S_o (cm^2/cc) (E+04)	$\bar{D}$ (μm)	ρ_a (g/ml)	ϕ_{Hg} (frac)	S_r (frac)	RE (frac)
Mean	0.0671	0.933	13.940	0.296	2.602	0.146	0.613	0.388
Median	0.0670	0.935	13.932	0.295	2.604	0.145	0.616	0.384
Min.	0.0614	0.830	12.482	0.260	2.551	0.138	0.559	0.339
Max.	0.0766	1.061	16.450	0.350	2.649	0.162	0.661	0.441
Q1	0.0637	0.861	12.716	0.274	2.588	0.142	0.578	0.362
Q3	0.0690	0.983	14.653	0.313	2.621	0.150	0.639	0.422
St. Dev.	0.0040	0.075	1.221	0.025	0.024	0.006	0.033	0.033

Table 3: Correlation Matrix for the Mercury Porosimetry Properties for Indiana Limestone Cores

	$V_{int.}$	SA	S_o	$\bar{D}$	ρ_a	ϕ_{Hg}	S_f
SA	0.257						
S_o	-0.429	0.762					
$\bar{D}$	0.538	-0.472	-0.786				
ρ_a	0.482	0.170	-0.182	0.365			
ϕ_{Hg}	0.723	0.387	-0.133	0.436	0.813		
S_f	0.499	-0.515	-0.818	0.734	0.420	0.291	
RE	-0.499	0.515	0.818	-0.734	-0.420	-0.291	-1.000

Table 4: Correlation Matrix for the Full Model for Indiana Limestone Cores at Breakthrough

	ϕ brine	K	τ	F	WI	S_{wi}	$V_{int.}$	SA	S_g	$\bar{D}$	ρ_g	ϕ Hg	RE	S_{or} @ B.T.
k	0.496													
τ	-0.682	-0.361												
F	-0.895	-0.445	0.936											
WI	0.188	-0.188	-0.061	-0.123										
S_{wi}	-0.050	0.166	0.095	0.070	-0.492									
$V_{int.}$	0.320	0.546	-0.203	-0.277	0.026	0.388								
SA	-0.126	0.155	0.253	0.226	-0.190	0.148	0.257							
S_g	-0.350	-0.230	0.391	0.416	-0.221	-0.096	-0.429	0.762						
$\bar{D}$	0.343	0.308	-0.399	-0.415	-0.037	0.280	0.538	-0.472	-0.786					
ρ_g	0.548	0.681	-0.427	-0.512	0.307	-0.164	0.482	0.170	-0.182	0.365				
ϕ_{Hg}	0.527	0.650	-0.416	-0.496	0.056	0.107	0.723	0.387	-0.133	0.436	0.813			
RE	-0.256	-0.572	0.443	0.393	-0.040	-0.081	-0.499	0.515	0.818	-0.734	-0.420	-0.291		
S_{or} @ B.T.	-0.404	-0.696	0.307	0.377	0.174	-0.581	-0.661	0.039	0.470	-0.611	-0.486	-0.564	0.644	
OR @ B.T.	0.481	0.747	-0.392	-0.461	0.022	0.253	0.646	-0.089	-0.516	0.613	0.660	0.636	-0.735	-0.932

B.T. = Breakthrough

Table 5: Correlation Matrix for the Full Model for Indiana Limestone Cores at Floodout

	ϕ brine	K	τ	F	WI	S_{wi}	V_{Hg}	SA	S_e	$\bar{D}$	ρ_e	ϕ Hg	RE	S_w @ F.O.
k	0.496													
τ	-0.682	-0.361												
F	-0.895	-0.445	0.936											
WI	0.188	-0.188	-0.061	-0.123										
S_{wi}	-0.050	0.166	0.095	0.070	-0.492									
V_{Hg}	0.320	0.546	-0.203	-0.277	0.026	0.388								
SA	-0.126	0.155	0.253	0.226	-0.190	0.148	0.257							
S_e	-0.350	-0.230	0.391	0.416	-0.221	-0.096	-0.429	0.762						
$\bar{D}$	0.343	0.308	-0.399	-0.415	-0.037	0.280	0.538	-0.472	-0.786					
ρ_e	0.548	0.681	-0.427	-0.512	0.307	-0.164	0.482	0.170	-0.182	0.365				
ϕ_{Hg}	0.527	0.650	-0.416	-0.496	0.056	0.107	0.723	0.387	-0.133	0.436	0.813			
RE	-0.256	-0.572	0.443	0.393	-0.040	-0.081	-0.499	0.515	0.818	-0.734	-0.420	-0.291		
S_w @ F.O.	-0.094	-0.581	-0.020	0.033	0.575	-0.800	-0.640	-0.363	0.071	-0.323	-0.177	-0.507	0.238	
OR @ F.O.	0.158	0.724	-0.045	-0.095	-0.493	0.474	0.703	0.408	-0.079	0.337	0.386	0.682	-0.334	-0.904

F.O. = Floodout

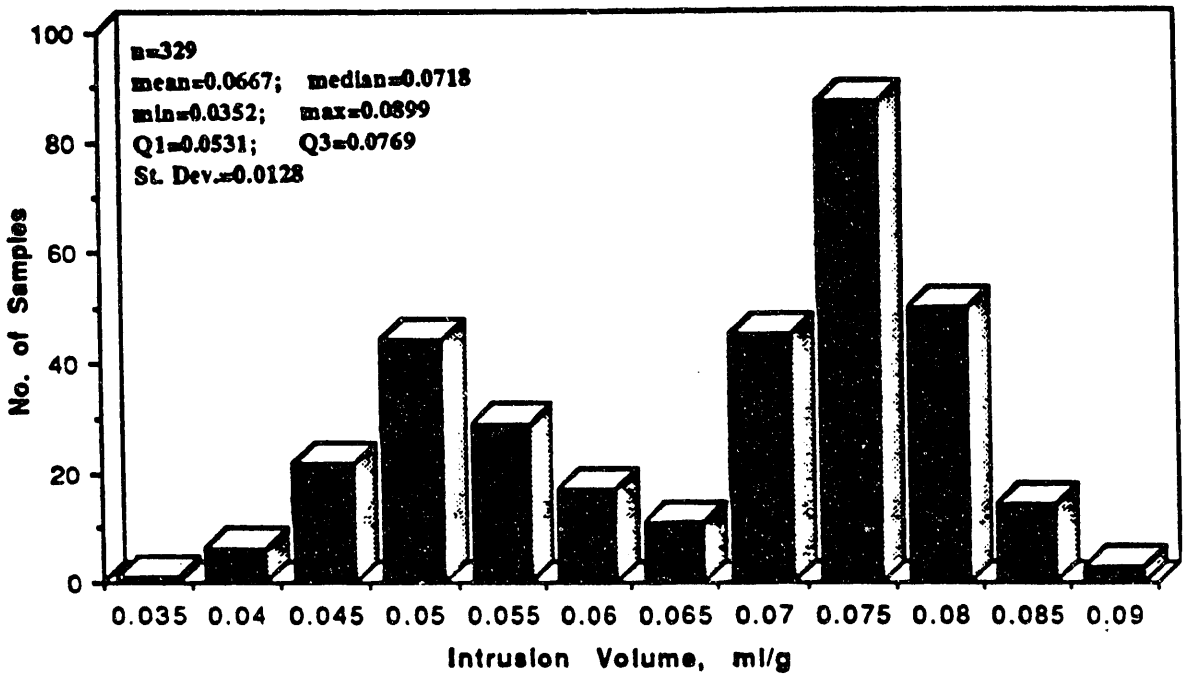

Fig. 1: Distribution of Total Intrusion Volume per Number of Indiana Limestone Core Plug Samples.

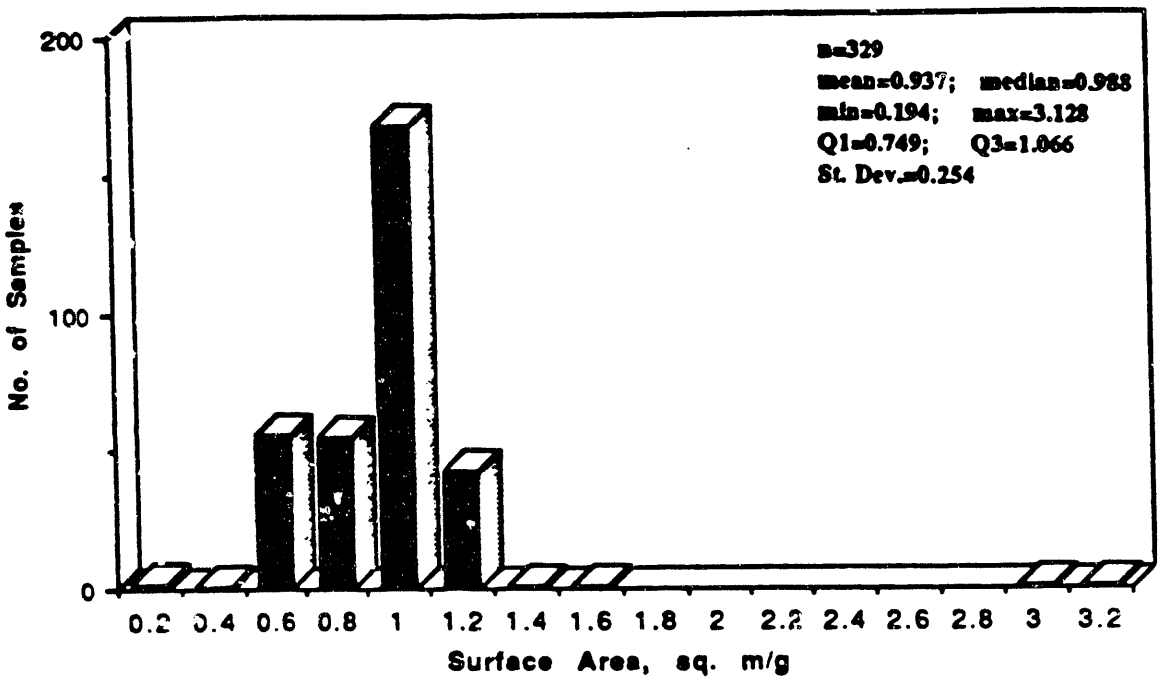

Fig. 2: Distribution of Total Surface Area per Number of Indiana Limestone Core Plug Samples.

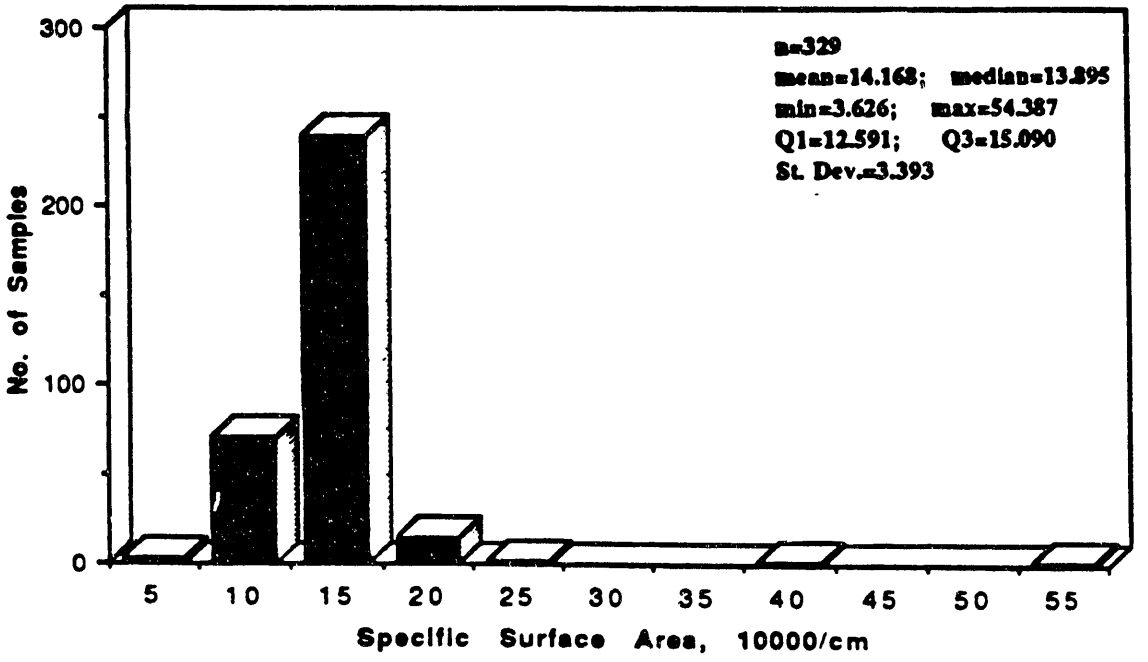

Fig. 3: Distribution of Specific Surface Area per Number of Indiana Limestone Core Plug Samples.

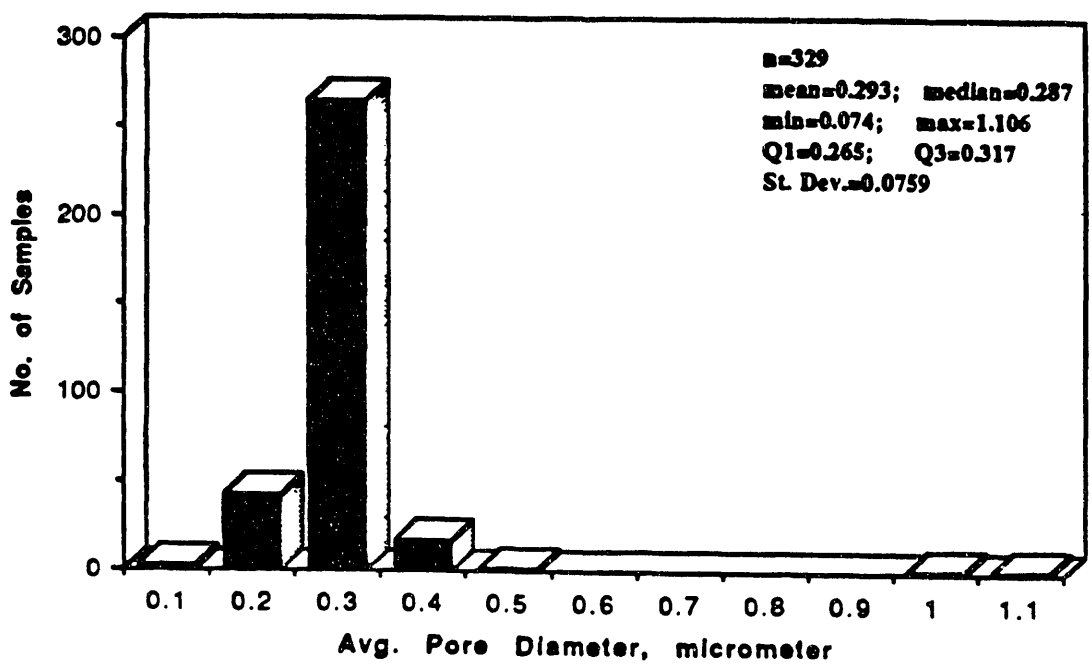

Fig. 4: Distribution of Average Pore Diameter per Number of Indiana Limestone Core Plug Samples.

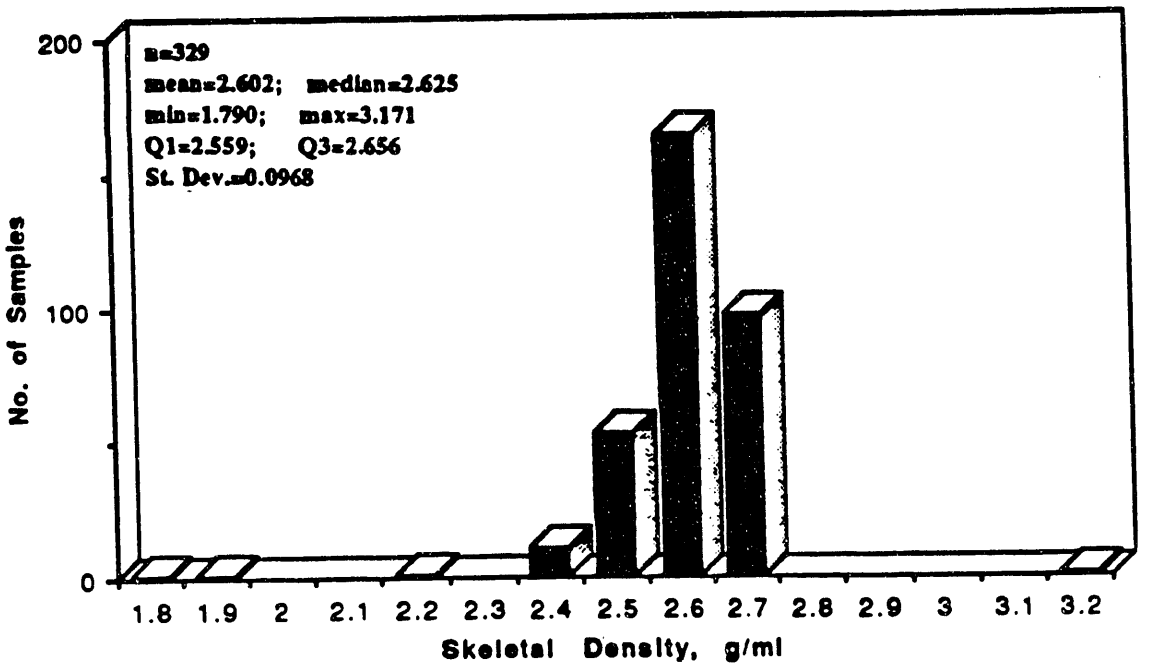

Fig. 5: Distribution of Apparent (Skeletal) Density per Number of Indiana Limestone Core Plug Samples.

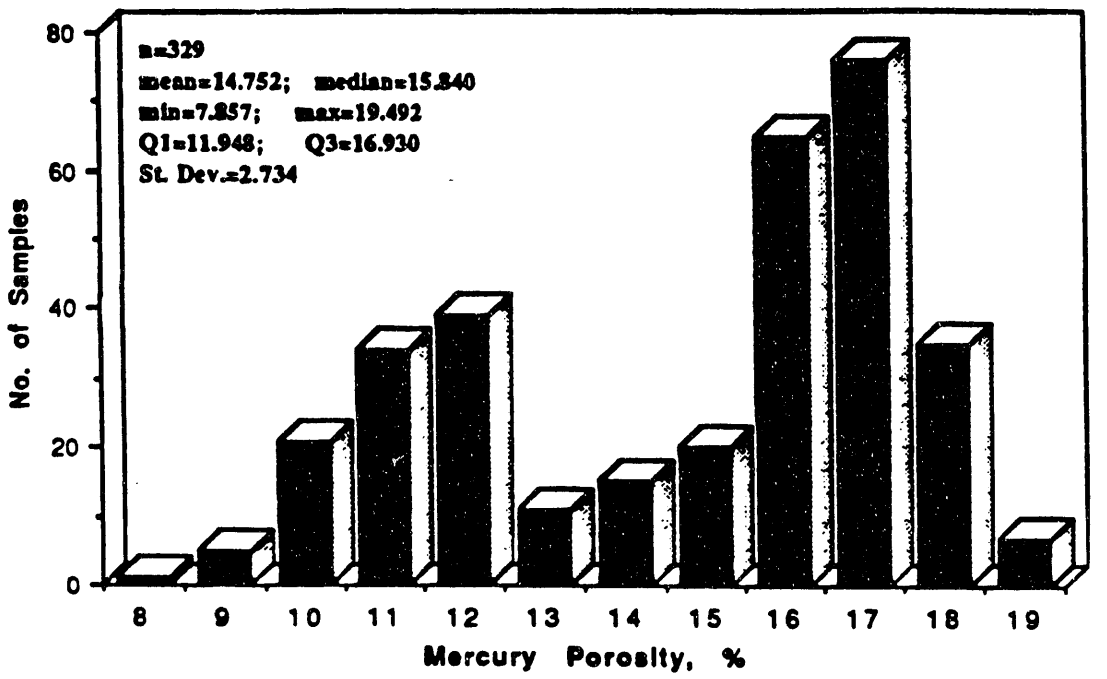

Fig. 6: Distribution of Mercury Porosity per Number of Indiana Limestone Core Plug Samples.

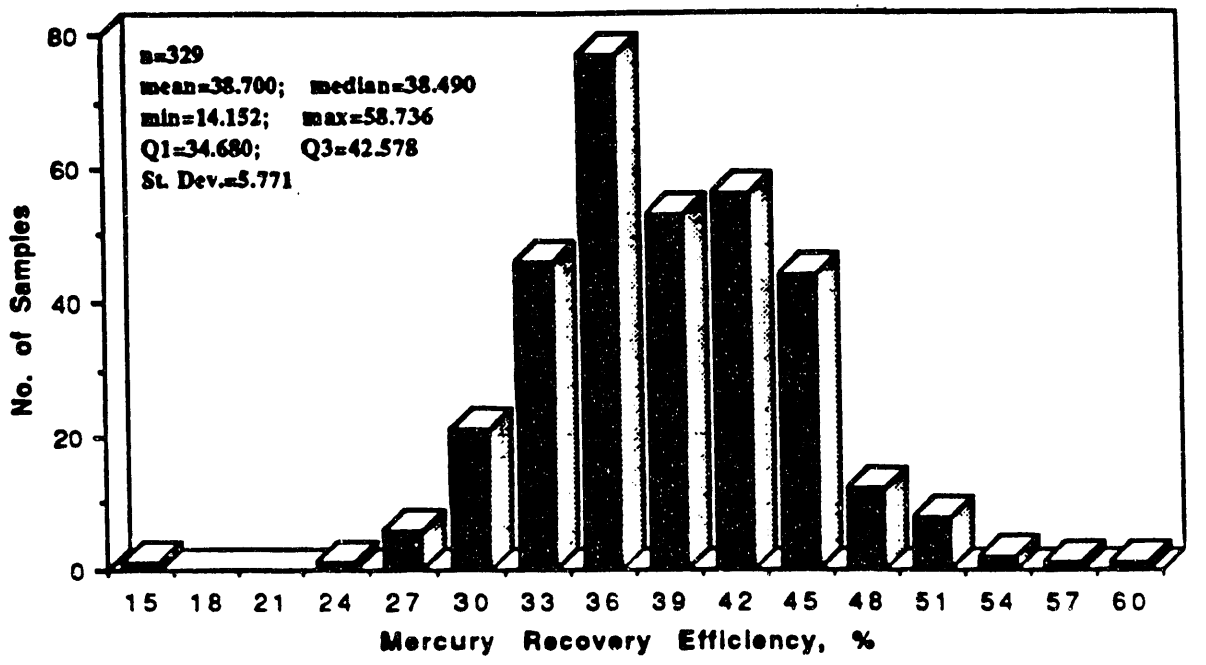

Fig. 7: Distribution of Mercury Recovery Efficiency per Number of Indiana Limestone Core Plug Samples.

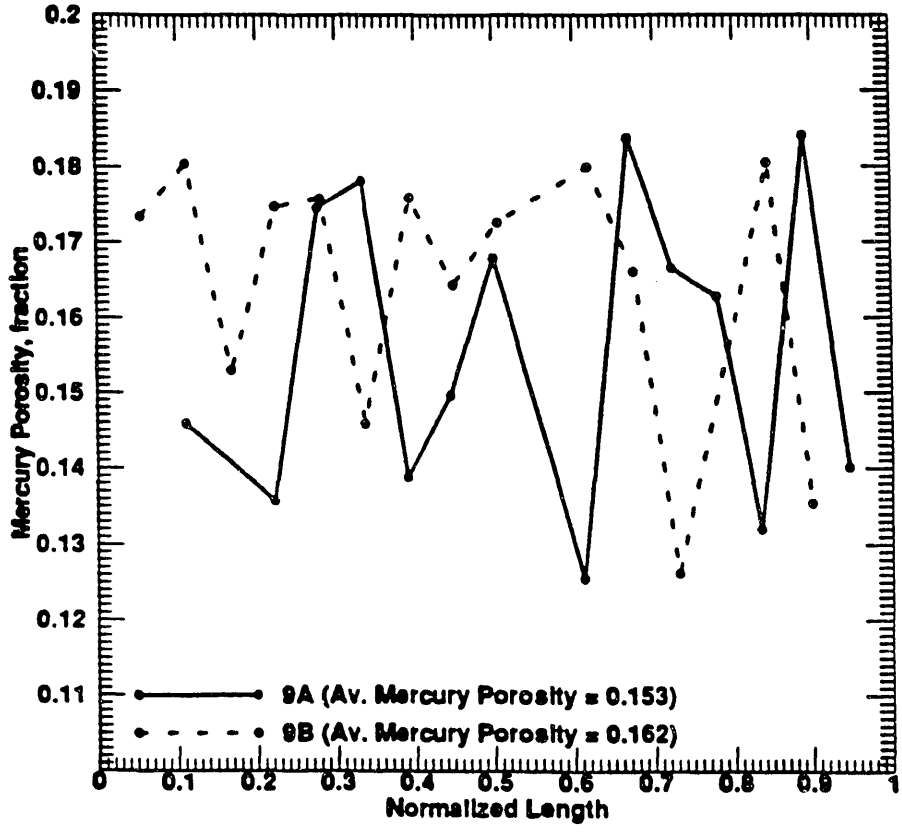

Fig. 8: Mercury Porosity vs. Normalized Length for Indiana Limestone Core Samples 9A and 9B.

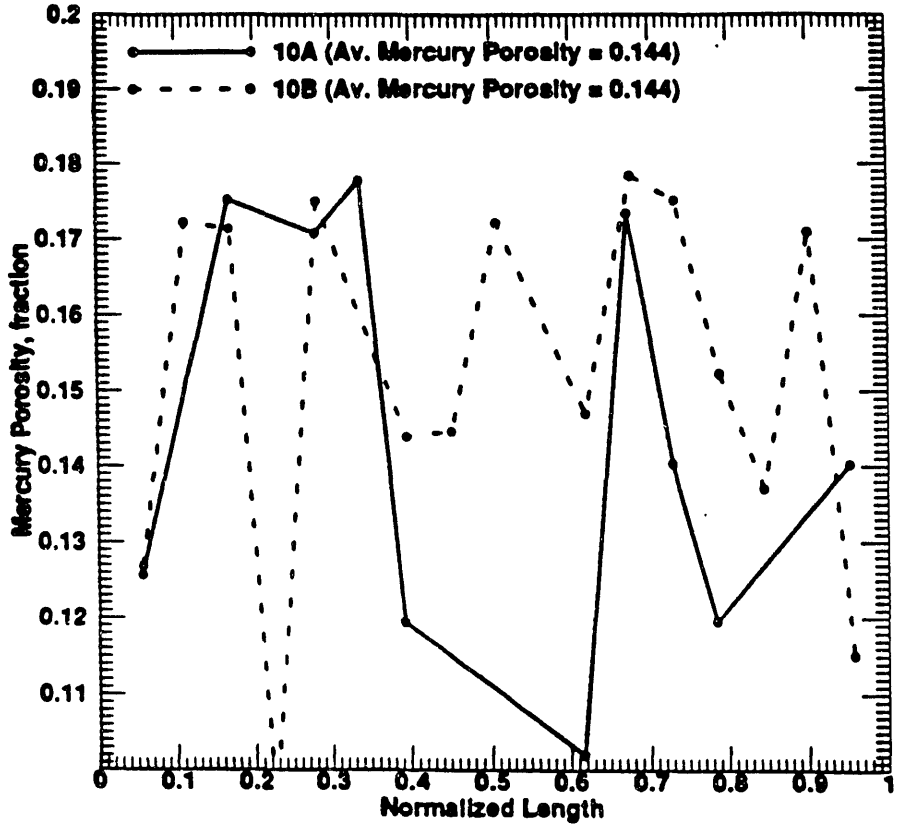

Fig. 9: Mercury Porosity vs. Normalized Length for Indiana Limestone Core Samples 10A and 10B.

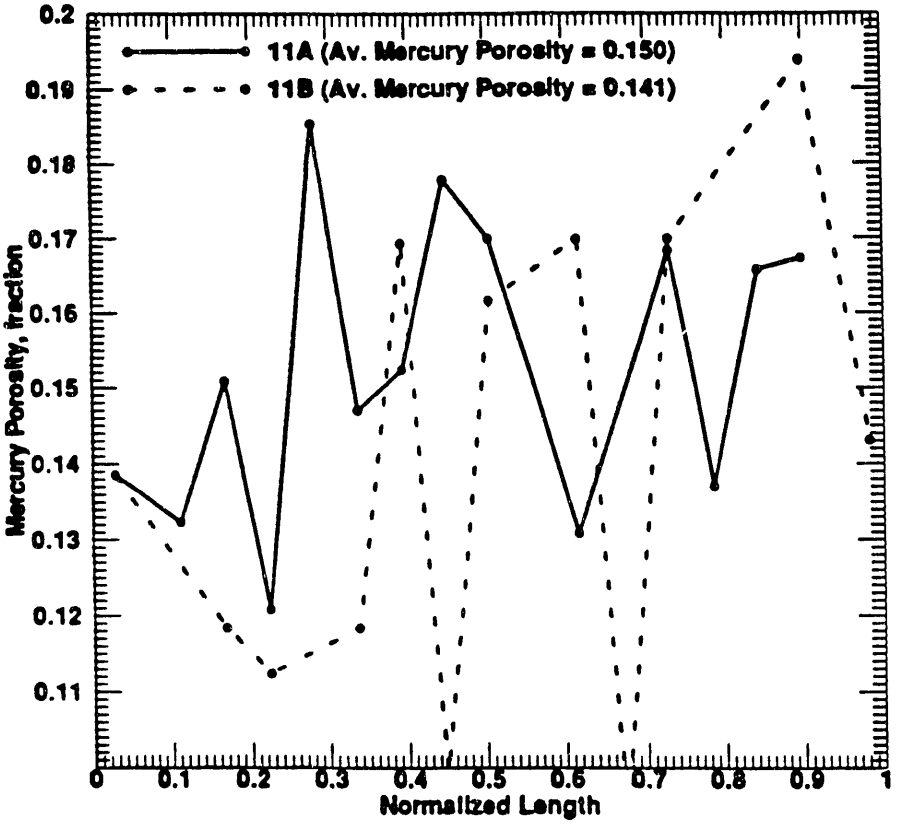

Fig. 10: Mercury Porosity vs. Normalized Length for Indiana Limestone Core Samples 11A and 11B.

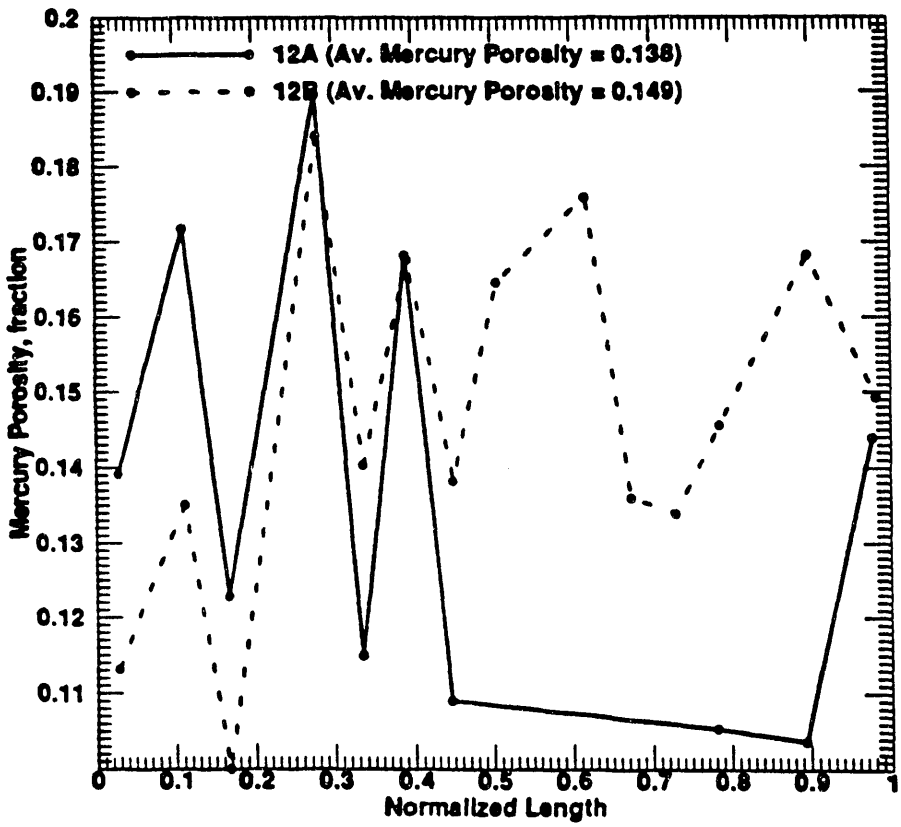

Fig. 11: Mercury Porosity vs. Normalized Length for Indiana Limestone Core Samples 12A and 12B.

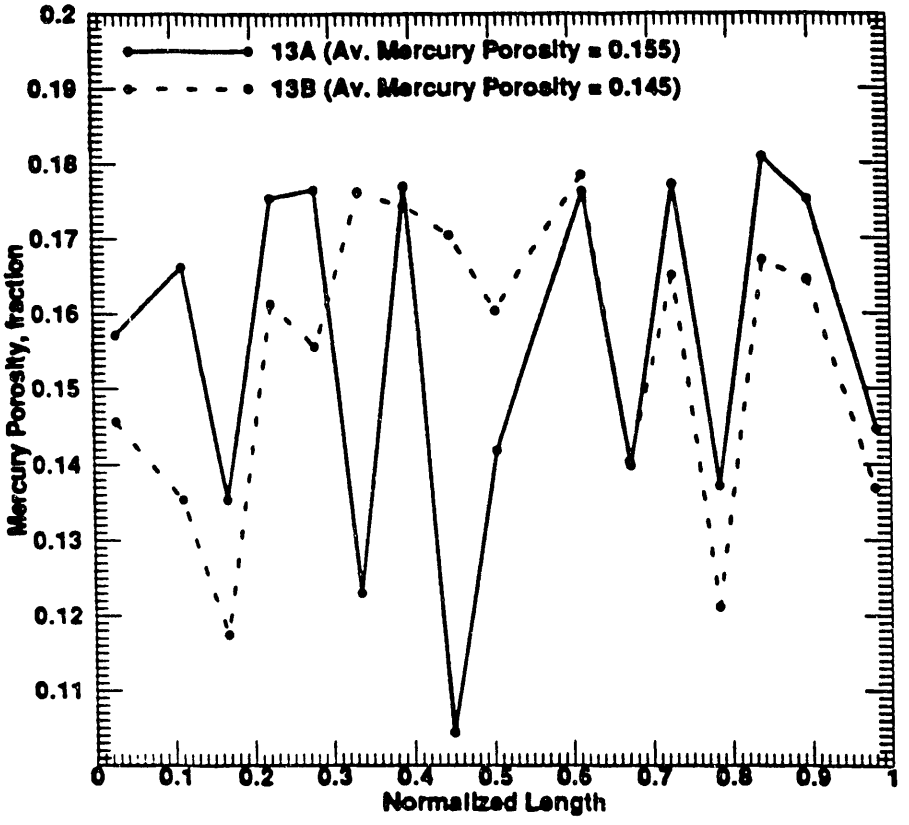

Fig. 12: Mercury Porosity vs. Normalized Length for Indiana Limestone Core Samples 13A and 13B.

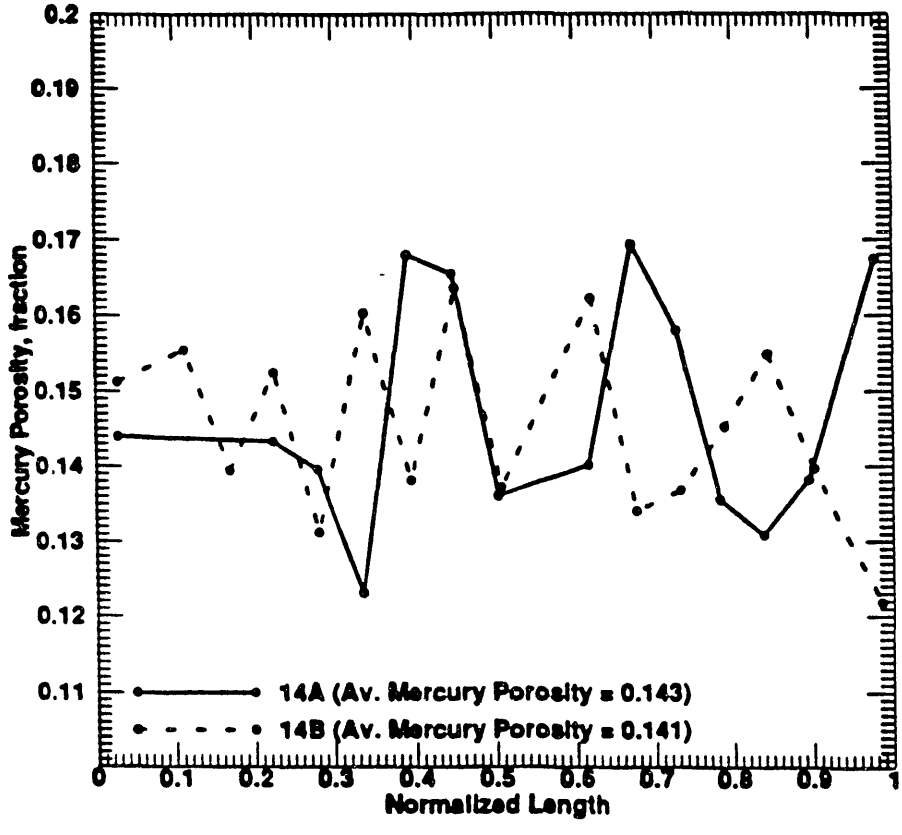

Fig. 13: Mercury Porosity vs. Normalized Length for Indiana Limestone Core Samples 14A and 14B.

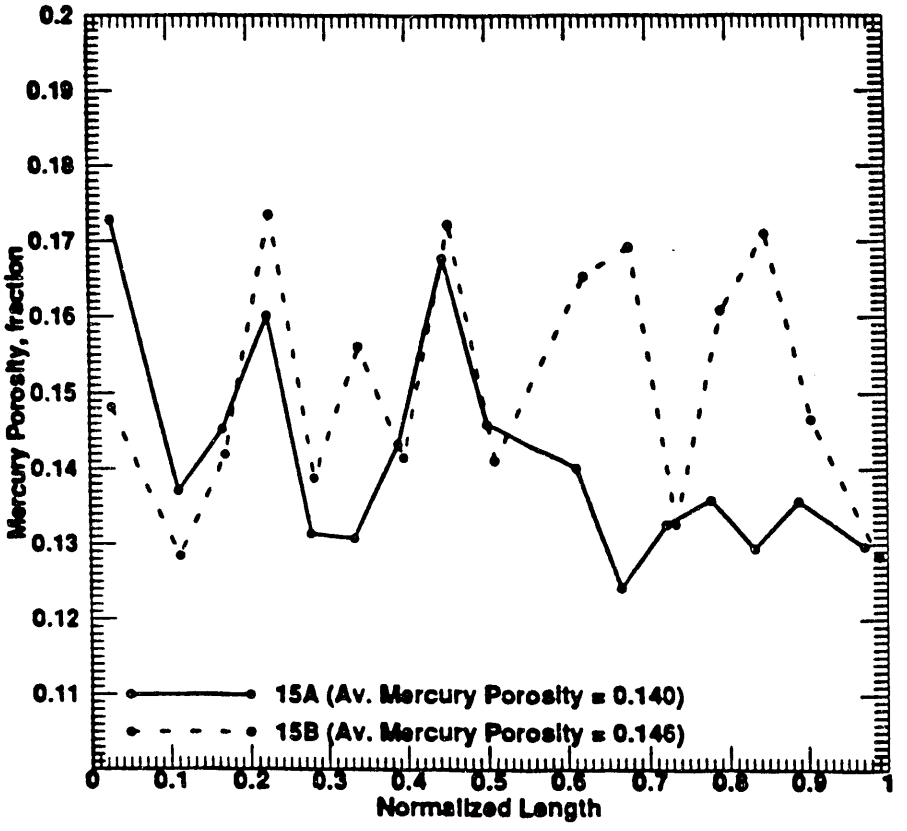

Fig. 14: Mercury Porosity vs. Normalized Length for Indiana Limestone Core Samples 15A and 15B.

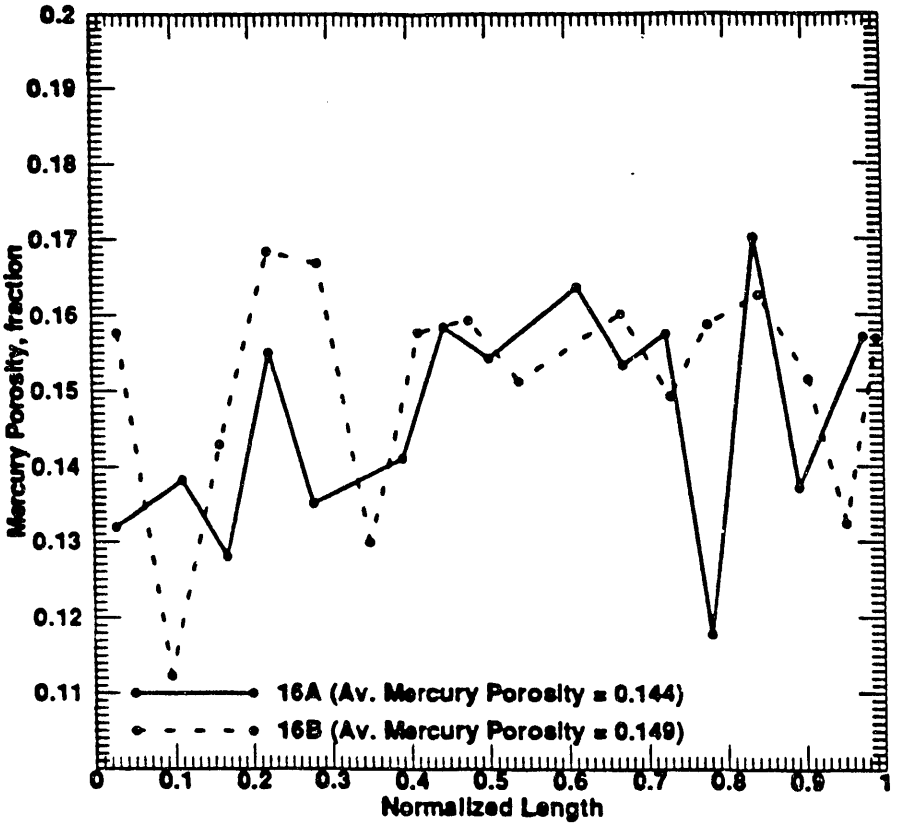

Fig. 15: Mercury Porosity vs. Normalized Length for Indiana Limestone Core Samples 16A and 16B.

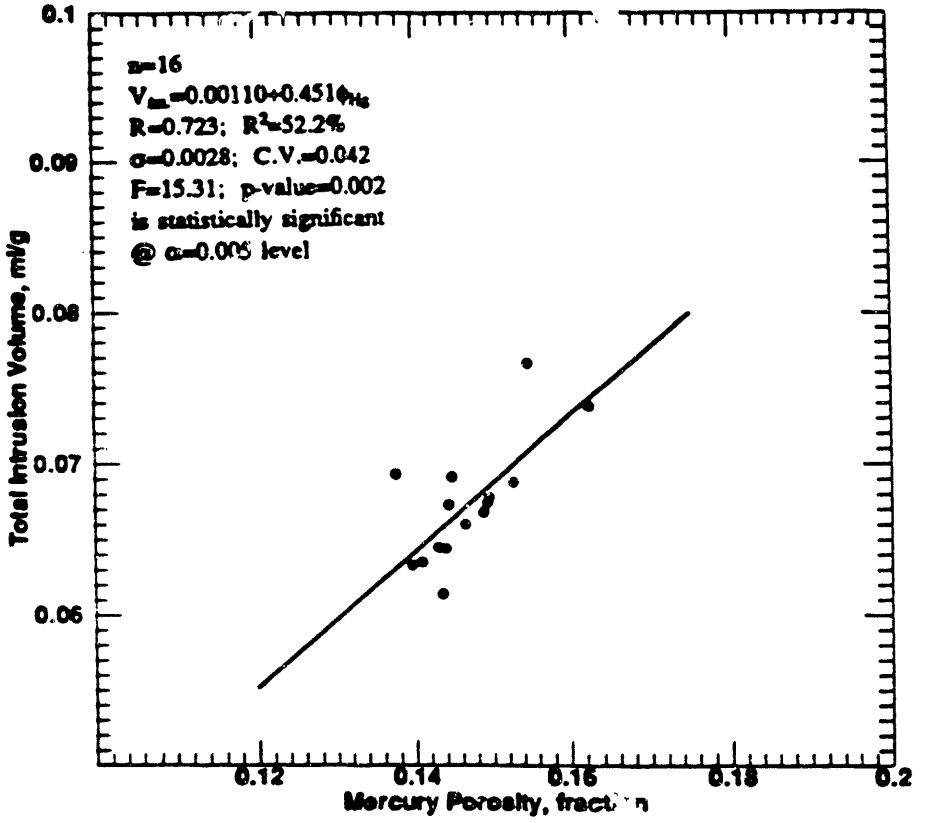

Fig. 16: Total Instrusion Volume vs. Mercury Porosity for Indiana Limestone Cores.

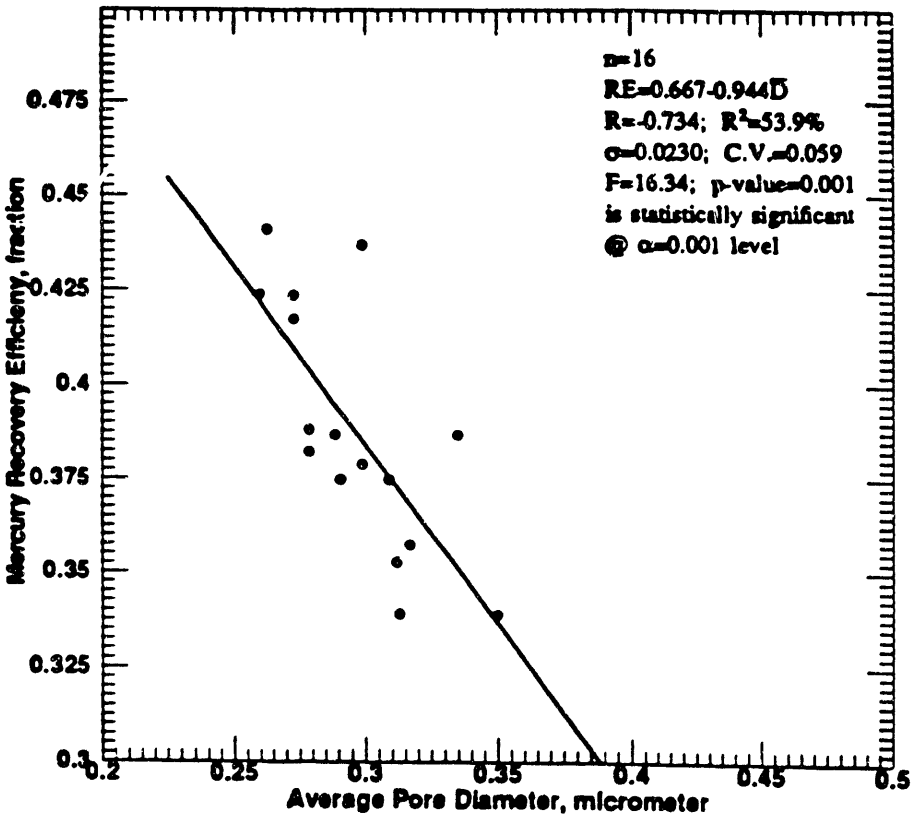

Fig. 17: Recovery Efficiency vs. Pore Diameter for Indiana Limestone Cores.

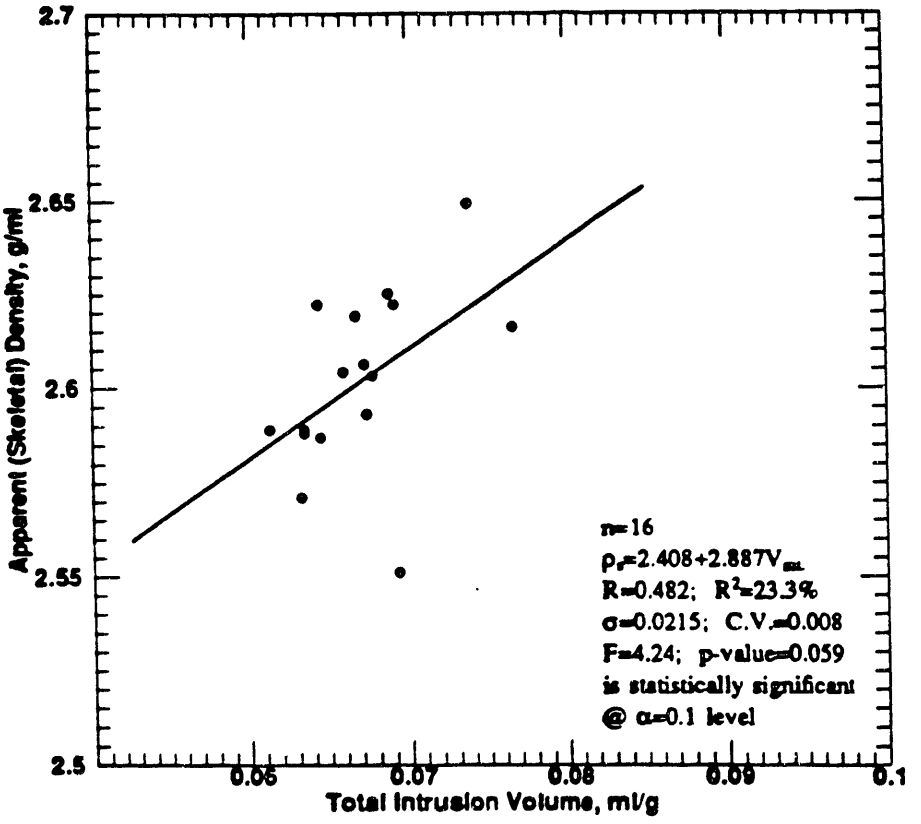

Fig. 18: Skeletal Density vs. Total Intrusion Volume for Indiana Limestone Cores.

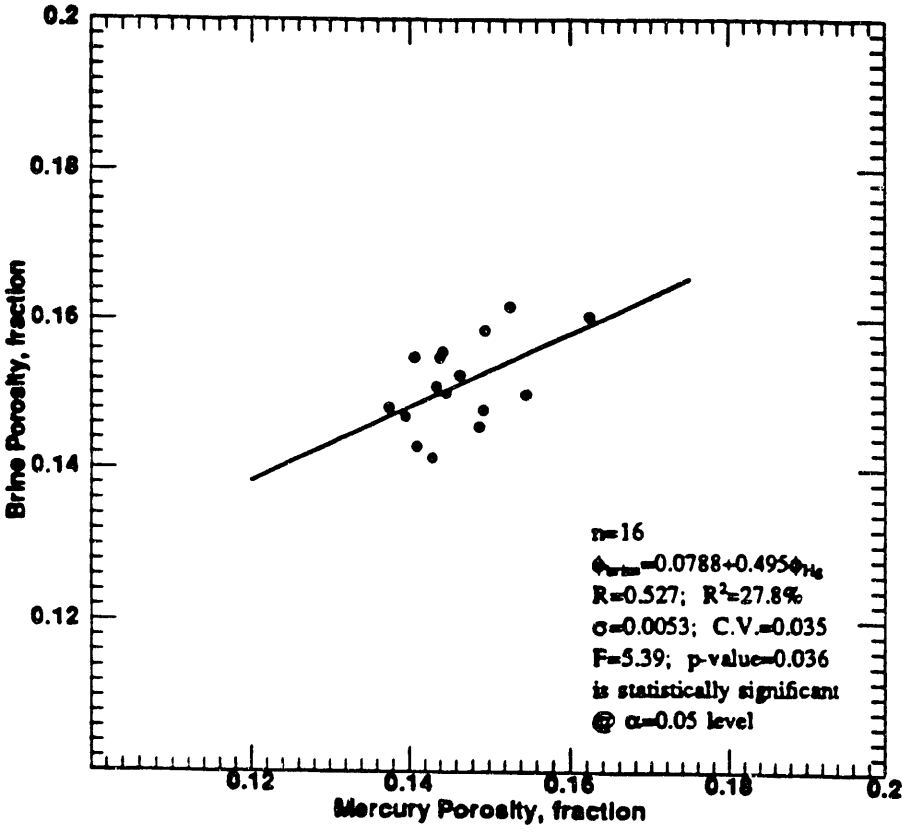

Fig. 19: Brine Porosity vs. Mercury Porosity for Indiana Limestone Cores.

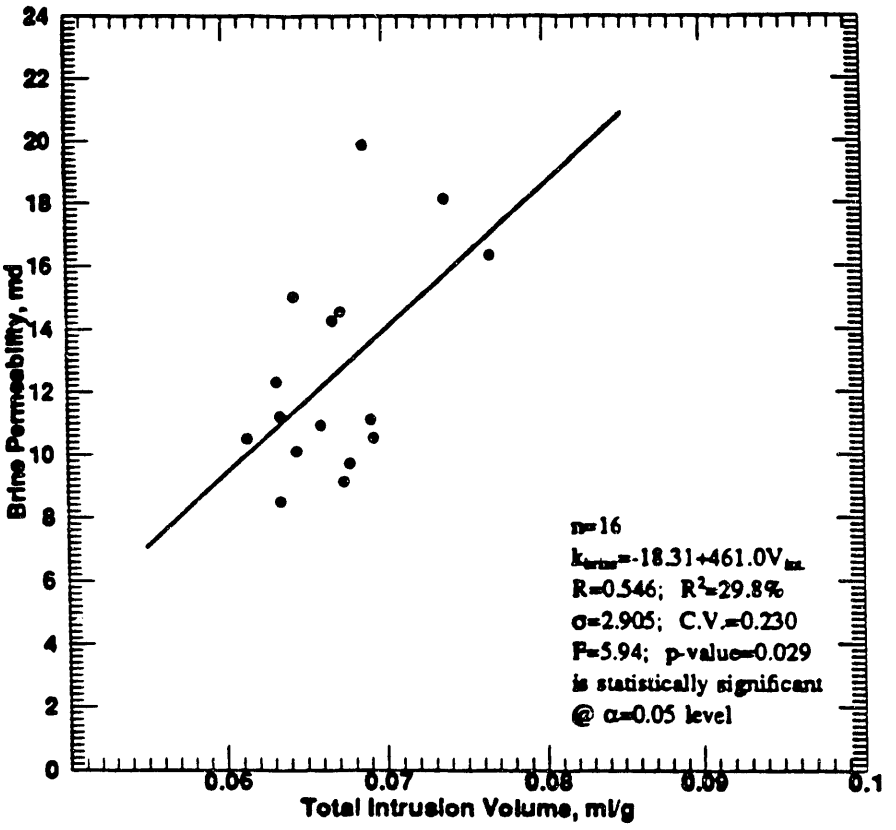

Fig. 20: Brine Permeability vs. Total Intrusion Volume for Indiana Limestone Cores.

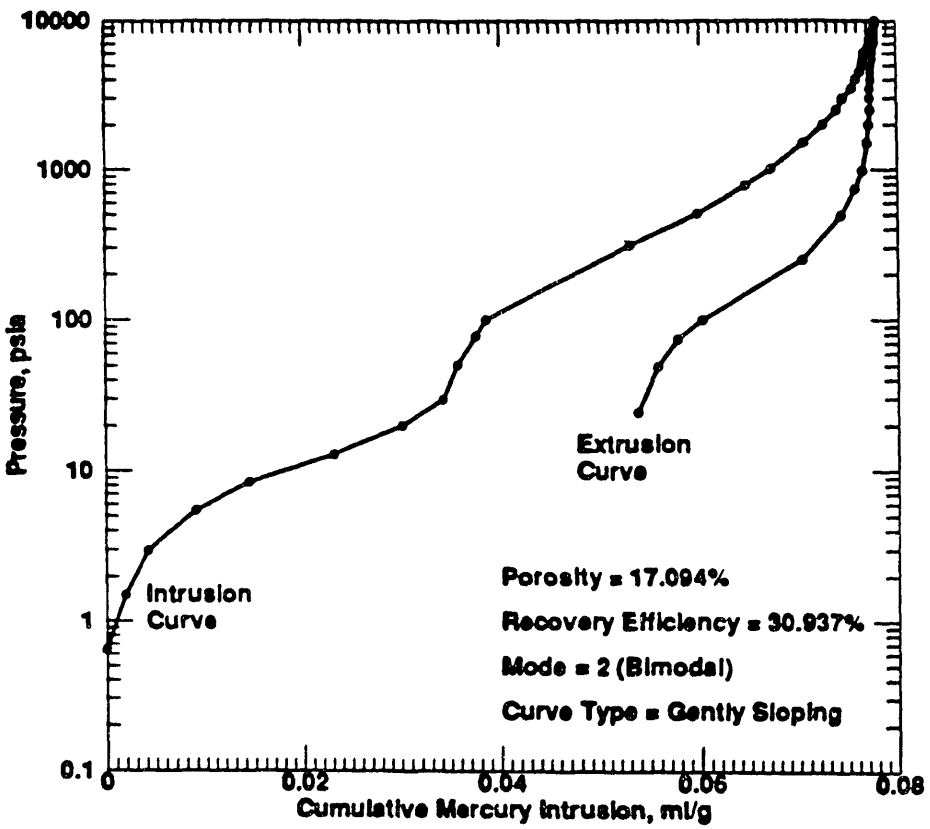

Fig. 21: Capillary Pressure vs. Cumulative Mercury Intrusion Curve for Indiana Limestone Core 15B - Plug 28.

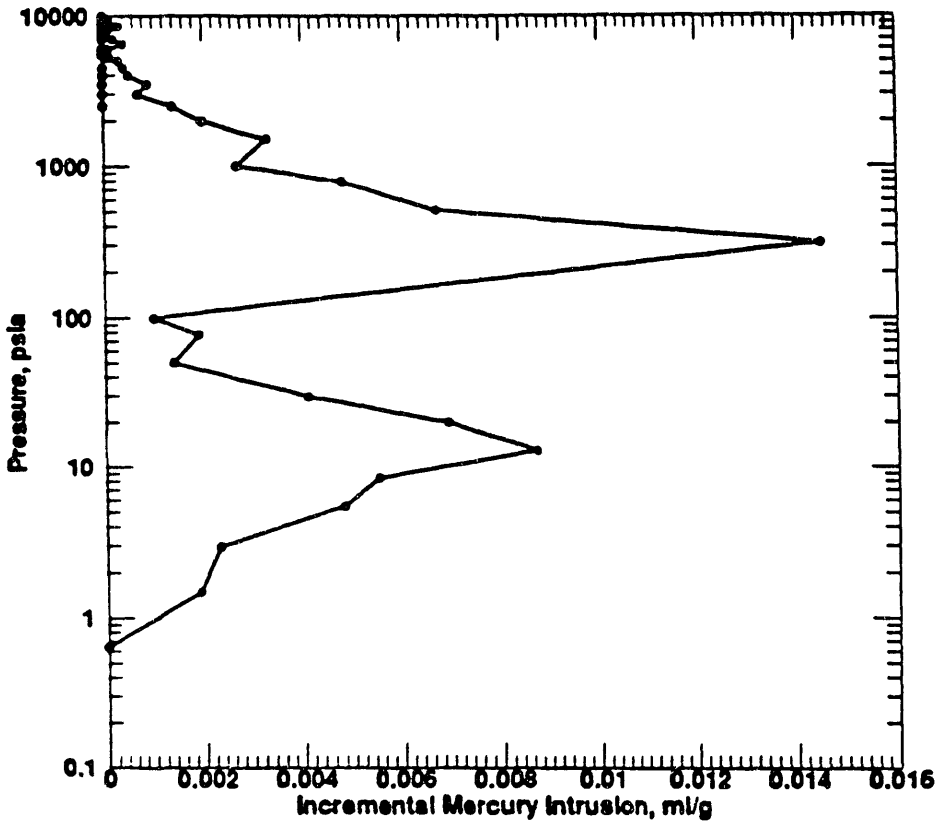

Fig. 22: Capillary Pressure vs. Incremental Mercury Intrusion Curve for Indiana Limestone Core 15B - Plug 28.

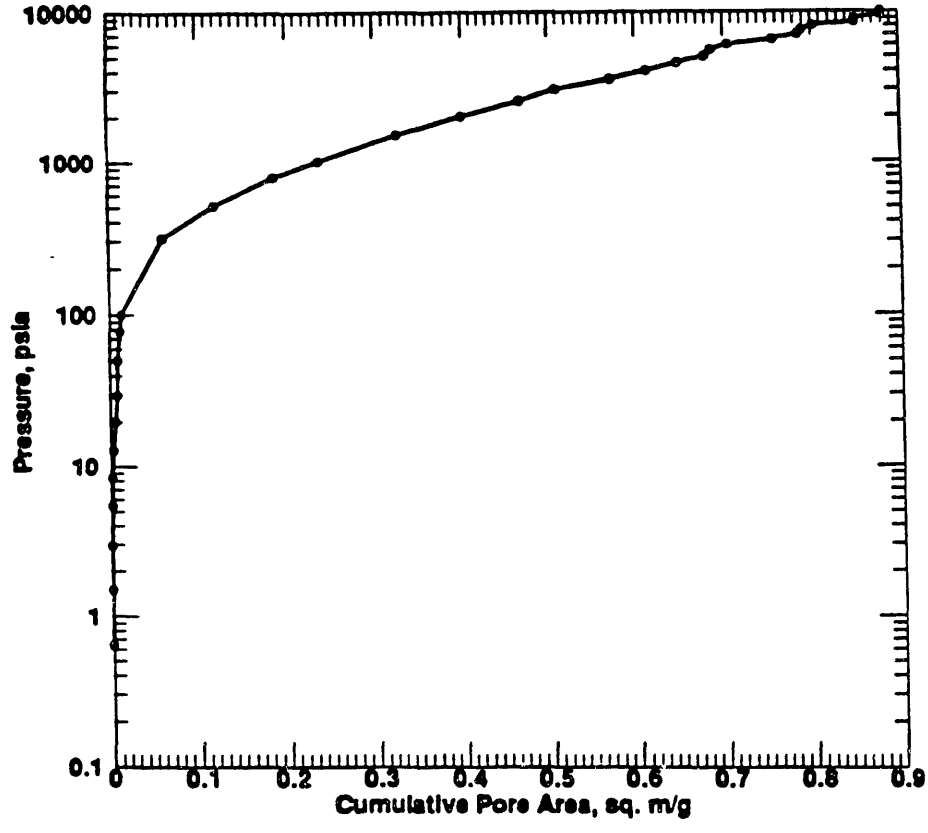

Fig. 23: Capillary Pressure vs. Cumulative Pore Area Curve for Indiana Limestone Core 15B - Plug 28.

DATE
FILMED
8/24/93
END